SI Appendix:

Structures of Qβ virions, virus-like particles, and the Qβ-MurA complex reveal internal coat proteins and the mechanism of host lysis

Zhicheng Cui [a], Karl V. Gorzelnik [a], Jeng-Yih Chang [a], Carrie Langlais [a,1], Joanita Jakana [b], Ry Young [a], Junjie Zhang [a,2]

[a] Department of Biochemistry and Biophysics, Center for Phage Technology, Texas A&M University, College Station, TX 77843

[b] National Center for Macromolecular Imaging, Verna and Marrs McLean Department of Biochemistry and Molecular Biology, Baylor College of Medicine, Houston, TX 77030

Movie Legends

Movie S1. Substrate binding causes the closure of the catalytic loop in MurA, which allows MurA to bind to the outer surface of A_2. The model for the open conformation of the *E. coli* MurA with no substrate bound was built using homology modeling based on the crystal structure of *Enterobacter cloacae* MurA (PDB ID: 1EJD).

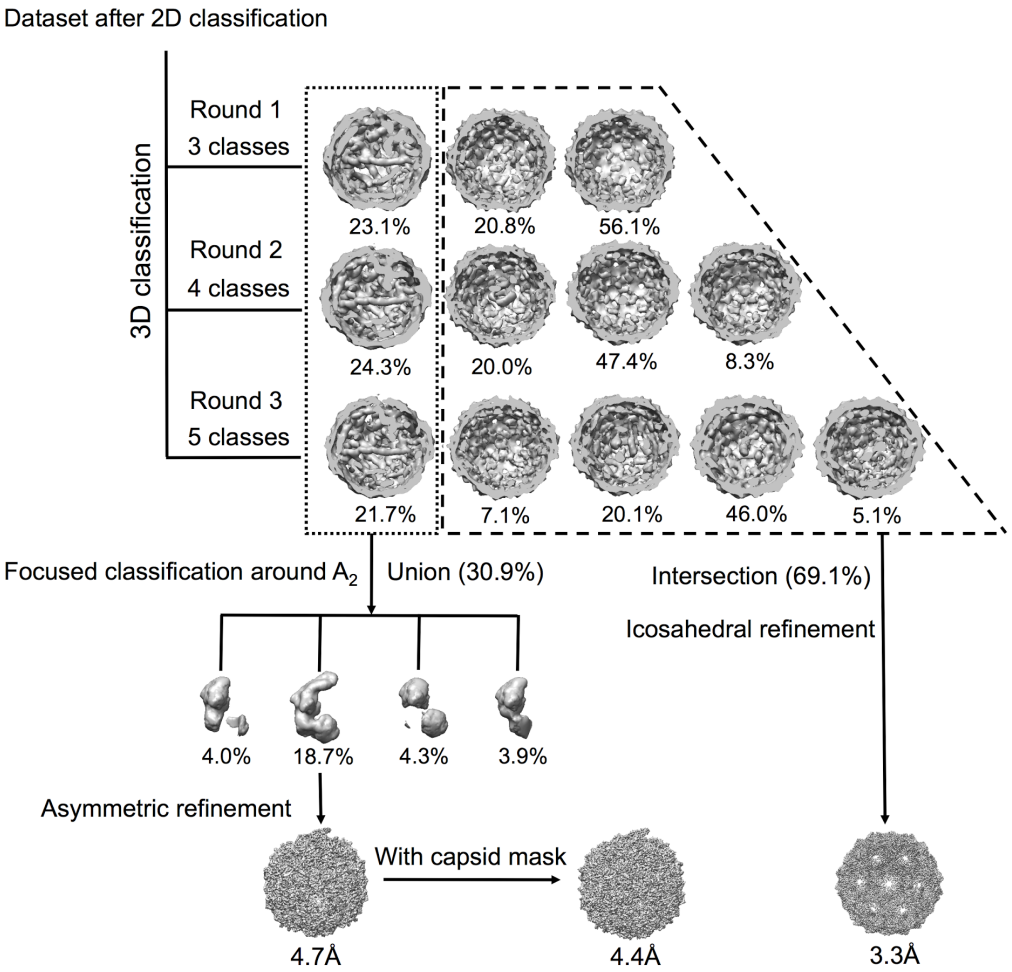

Figure S1. 3D classification of the Qβ image data. For the dataset screened after 2D classification, 30 iterations of the 3D classification was first performed for three independent rounds in Relion, requesting 3, 4 and 5 number of classes, respectively. For each round of the 3D classifications, one class showed defined densities of A_2 and the gRNA (outlined in a dotted rectangle). Particles within this class in each of the three rounds were combined as a union set with duplicate particles eliminated. This yielded about 30.9% of the total particles, which were subjected to another round of focused classification for 50 iterations around A_2. Finally, 18.7% of the particles showed good A_2 density, and particles in this class, corresponding to the Qβ virions, were asymmetrically refined to 4.7-Å resolution. The resolution was improved to 4.4Å after excluding the gRNA density during the final map refinement. The remaining particles in those classes that did not show a defined density for A_2 or RNA (outlined in a dashed trapezoid) turned out to have a perfect icosahedral capsid, corresponding to the virus-like particles (VLP). These VLPs from each round of the 3D classifications were combined as an intersection set, sharing only 69.1% of the total particles, and refined to 3.3-Å resolution with an icosahedral symmetry applied.

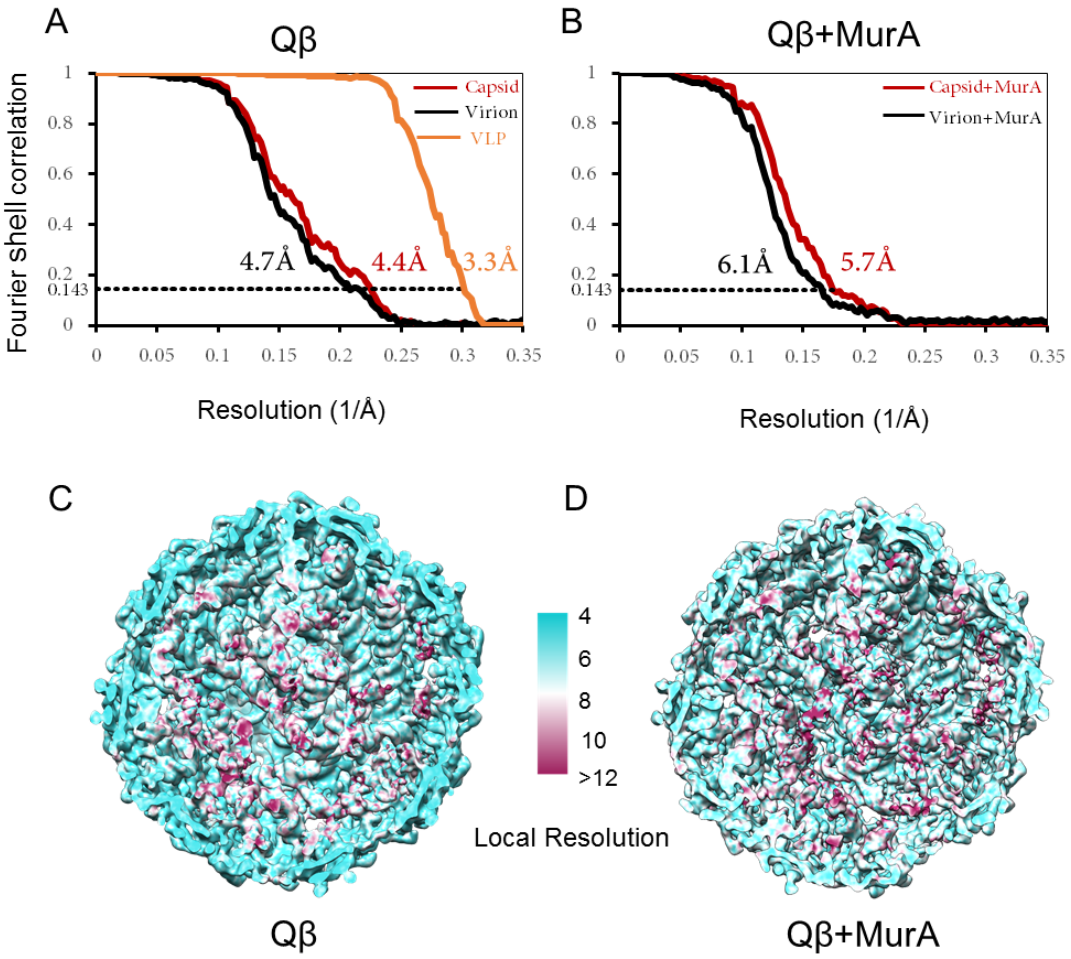

Figure S2. Resolution estimations. (A-B) Fourier shell correlation (FSC) of cryo-EM reconstructions of the Qβ virion, Qβ VLP and Qβ bound with MurA showing the overall resolutions based on the gold-standard criteria. The FSC curves for the complete virion, VLP and the virion capsid without the gRNA are in black, orange and red, respectively. (C-D) Cutaway view of each reconstruction showing the local resolution. The color scale indicates the local resolution. The map for Qβ alone is low-pass filtered to 6Å to better visualize the gRNA.

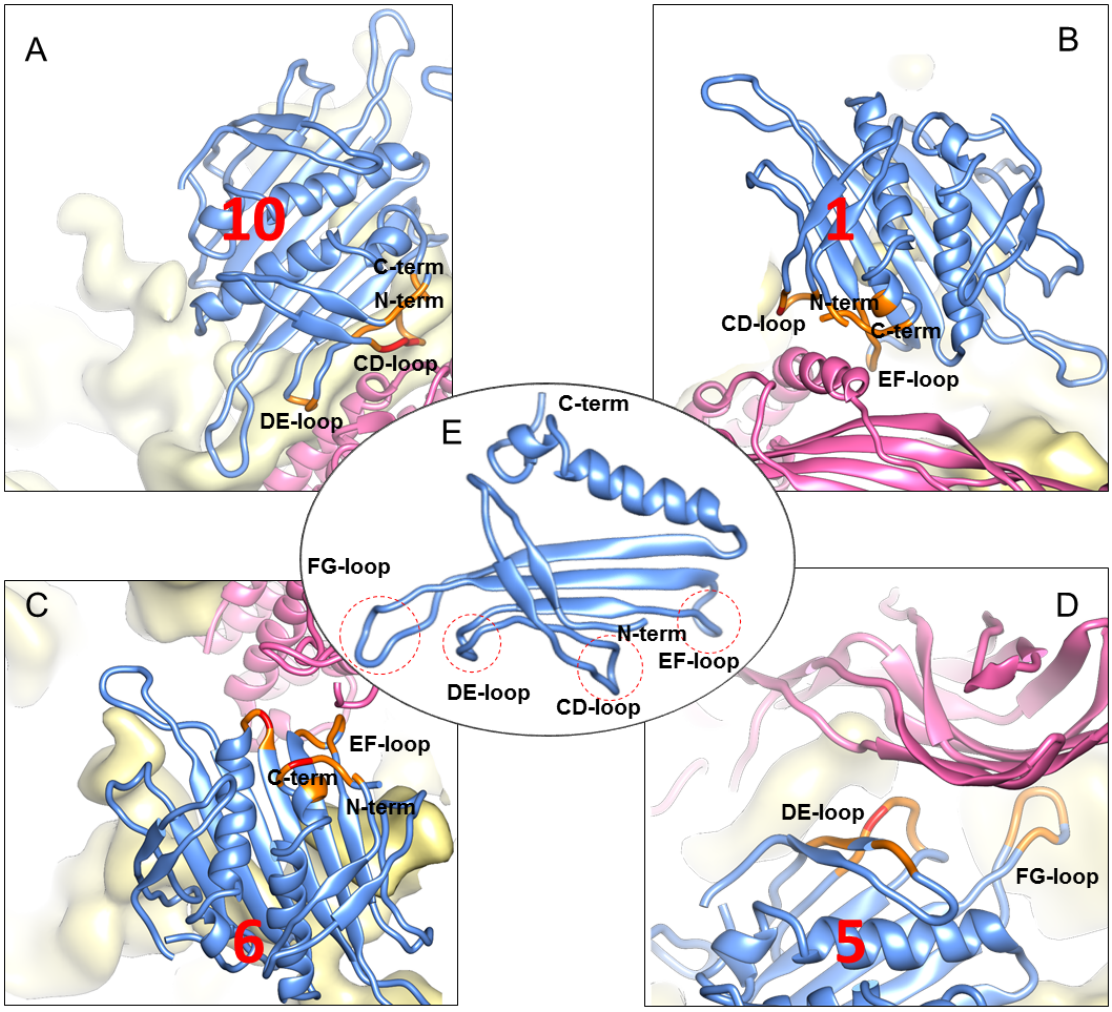

Figure S3. Interactions between Qβ coat protein dimers and A_2. Residues of the coat proteins within 5Å and 10Å Cα-Cα distances to A_2 are colored red and orange, respectively. The numbering for the coat protein dimers follows Figure 1. (A) For coat protein dimer 10, its N-terminus (residues 2-4), CD-loop (residues 23-35), DE-loop (residues 40-43) and C-terminus (residues 131-132) interact with the N-terminal end of α-helix 9 (residue 389-400), the N-terminal end of β-strand 12 (residues 340-344) and the C-terminal end of β-strand 11 (residues 280-283) of A_2. (B) For coat protein dimer 1, its N-terminus (residues 1-2), CD-loop (residues 26-32), EF-loop (residues 52-57) and C-terminus (residues 127-132) interact with α-helix 2 (residues 129-146) of A_2. (C) For coat protein dimer 6, its EF-loop (residues 54-57 and residues 59-60), the C-terminal of β-strand G (residues 97-101) and N-terminus (residues 123-130) interact with N-terminus (residues 3, residues 10-16) and the N-terminal end of α-helix 6 (residues 289-290 and 292-294) of A_2. (D) For coat protein dimer 5, its AB-loop (residues 16-18), β-strand B (residues 20-22), DE-loop (residues 36-42), and FG-loops (residue 75-76 and 79-82) interact with β-strand 5 (residues 51-53), the N-terminal end of β-strand 4 (residues 34-38), β-strand 9 (residues 114-116), β-strand 8 (residues 92-96), β-strand 13 (residues 372-379), and β-strand 12 (residues 355-358) of A_2. (E) A single copy of the coat protein with the loops and termini annotated.

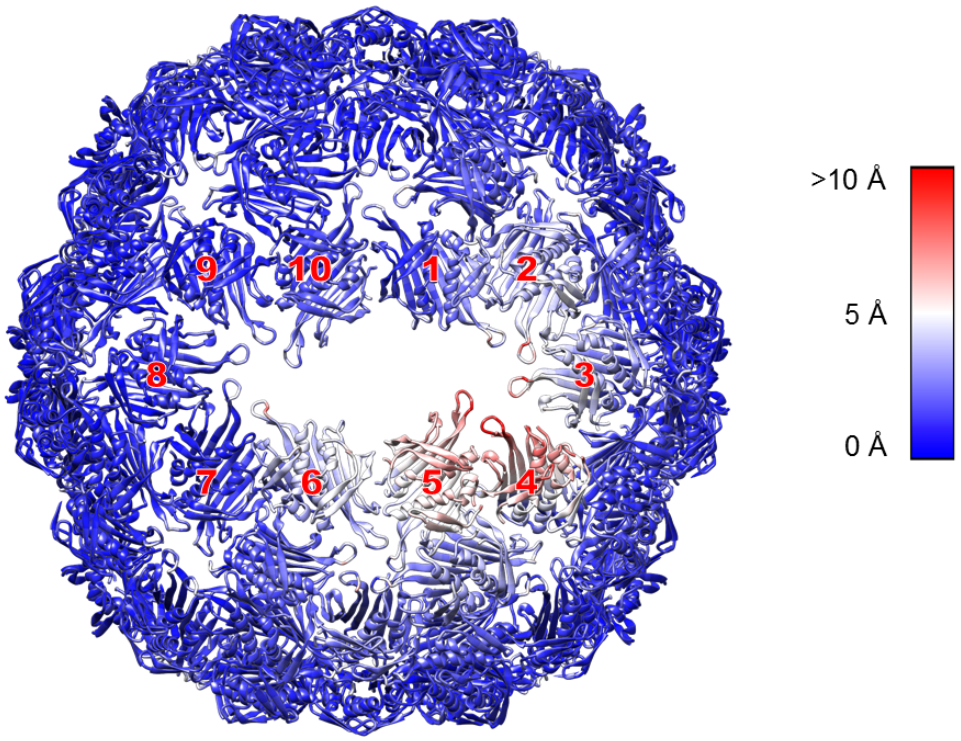

Figure S4. Conformational deviations of the corresponding Qβ coat proteins in the mature virion versus the virus-like particles (VLP). Coat protein dimers around the capsid opening are labeled as in Figure 1. The displacement of coat protein dimers in the mature virion compared to VLP is shown through a color scale. Coat protein dimers 2-6 are the most displaced in the mature virion compared to the virus-like particles, with some loop residues being displaced more than 10Å.

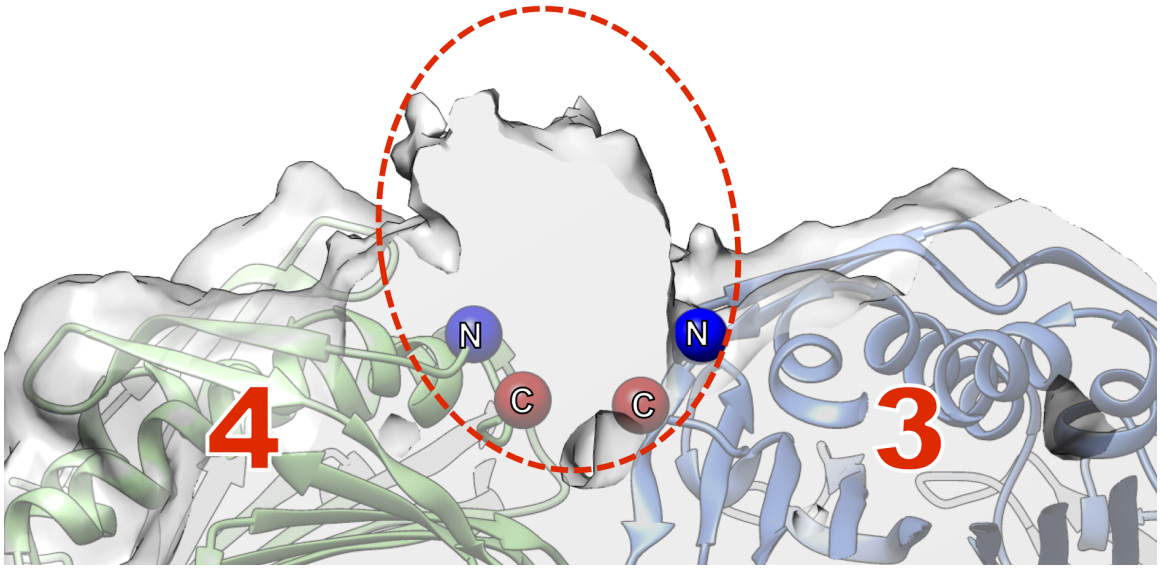

Figure S5. Extra electron density at the interface between the models of Qβ coat protein dimers 3 and 4. The N- and C-termini of the adjacent coat protein models at the interface are labeled as blue and red spheres, respectively. The extra density (from the unfiltered map of the Qβ virion) not occupied by the models of the coat proteins is marked by the red dashed oval.

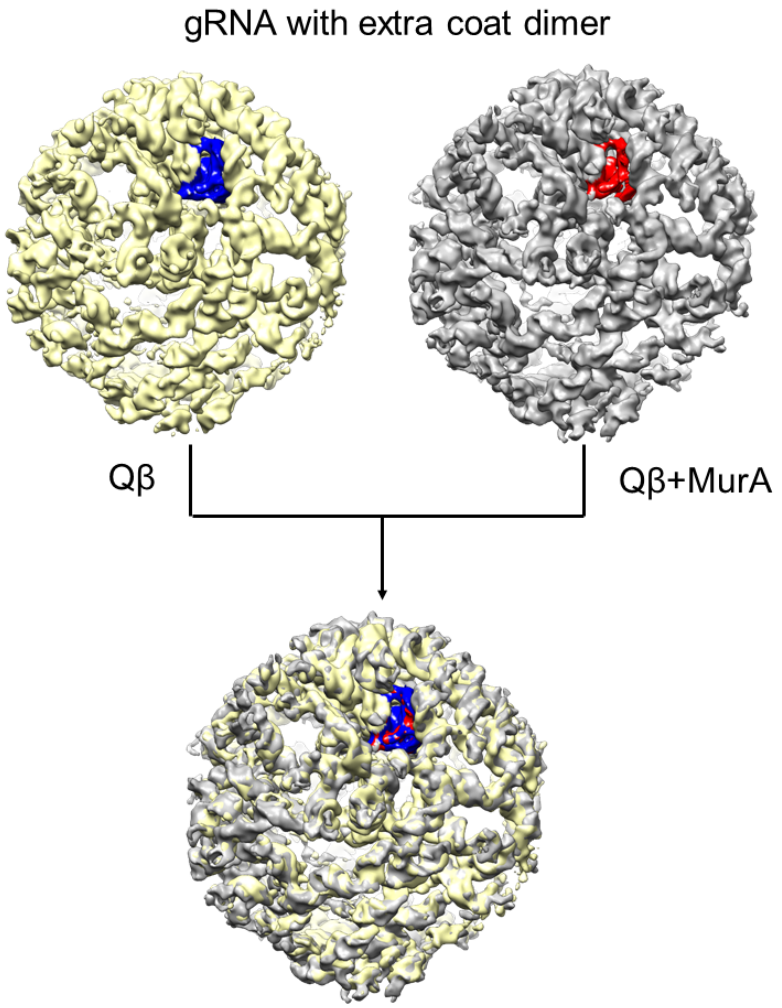

Figure S6. Structural comparison of the gRNA and the sequestered coat protein dimer between Qβ and Qβ+MurA. The protein capsid is removed (except for the sequestered coat protein dimer) and the gRNA is colored yellow and gray for Qβ alone and Qβ bound with MurA, respectively. The density for the sequestered coat protein dimer is colored blue and red in Qβ alone and Qβ bound with MurA, respectively. When the electron density maps are superimposed, there are no major differences between the two maps. The density from the Qβ alone map is low-pass filtered to 6-Å resolution.

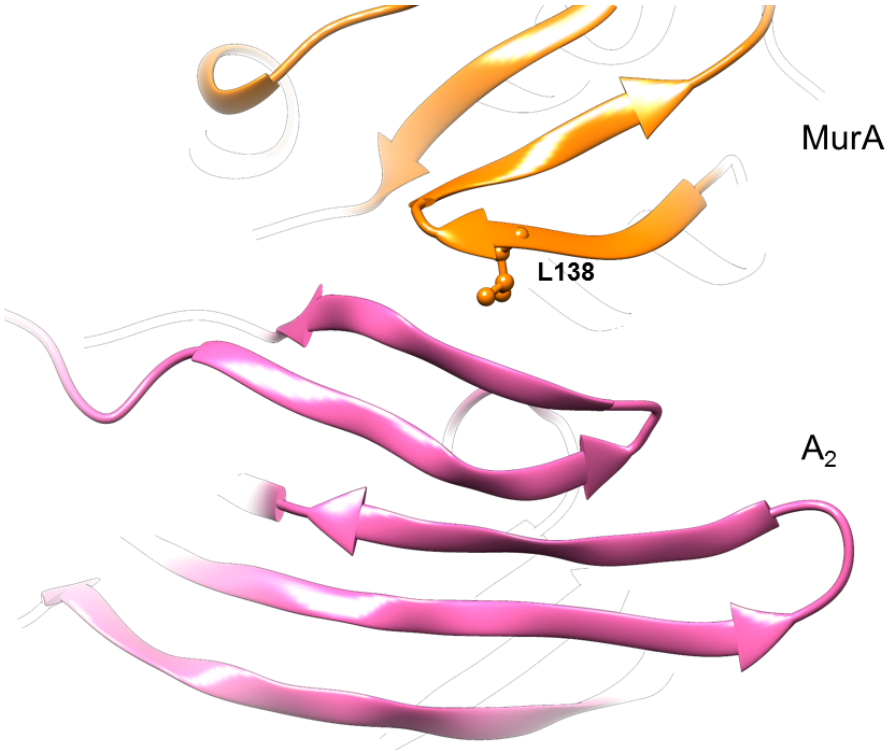

Figure S7. The interaction between the β-sheets from MurA and A_2. MurA is colored orange while A_2 is hot pink. Leu138, the residue with its mutation in MurA causing resistance to A_2, is labeled as a ball-and-stick model.

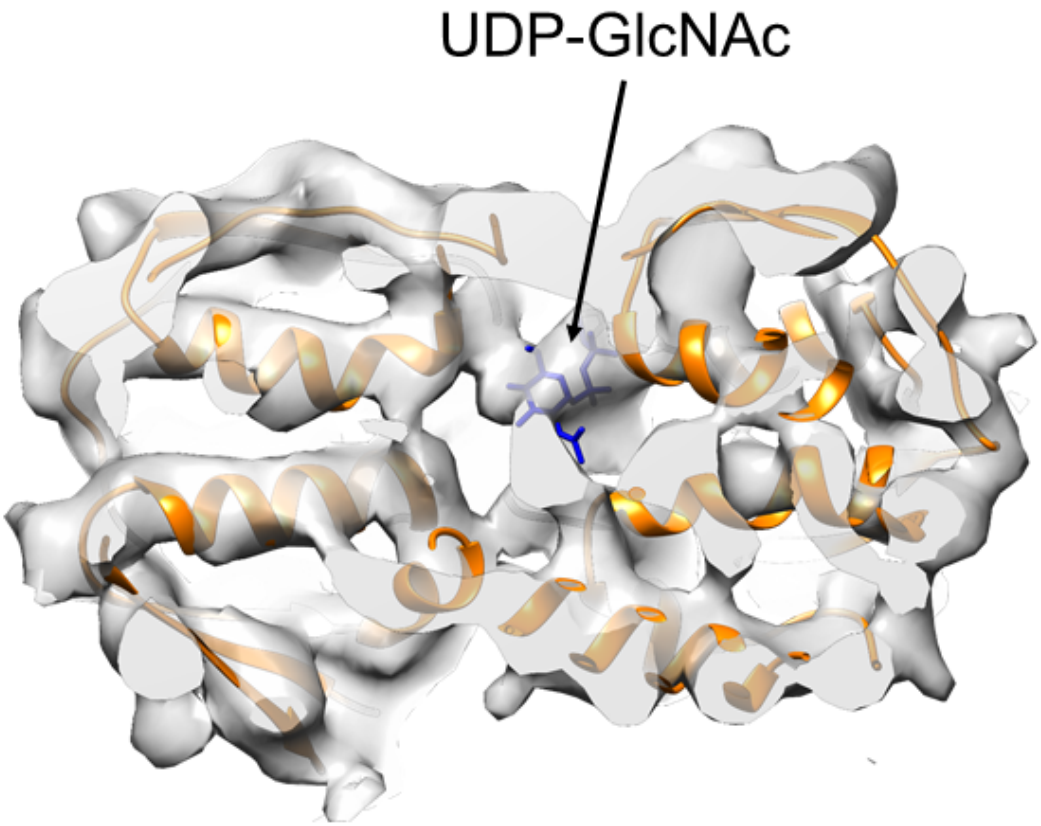

Figure S8. Slice view of the density for MurA from the MurA-Qβ complex. The models of MurA (orange) and its substrate UDP-GlcNAc (blue) fit well into the density (transparent gray).

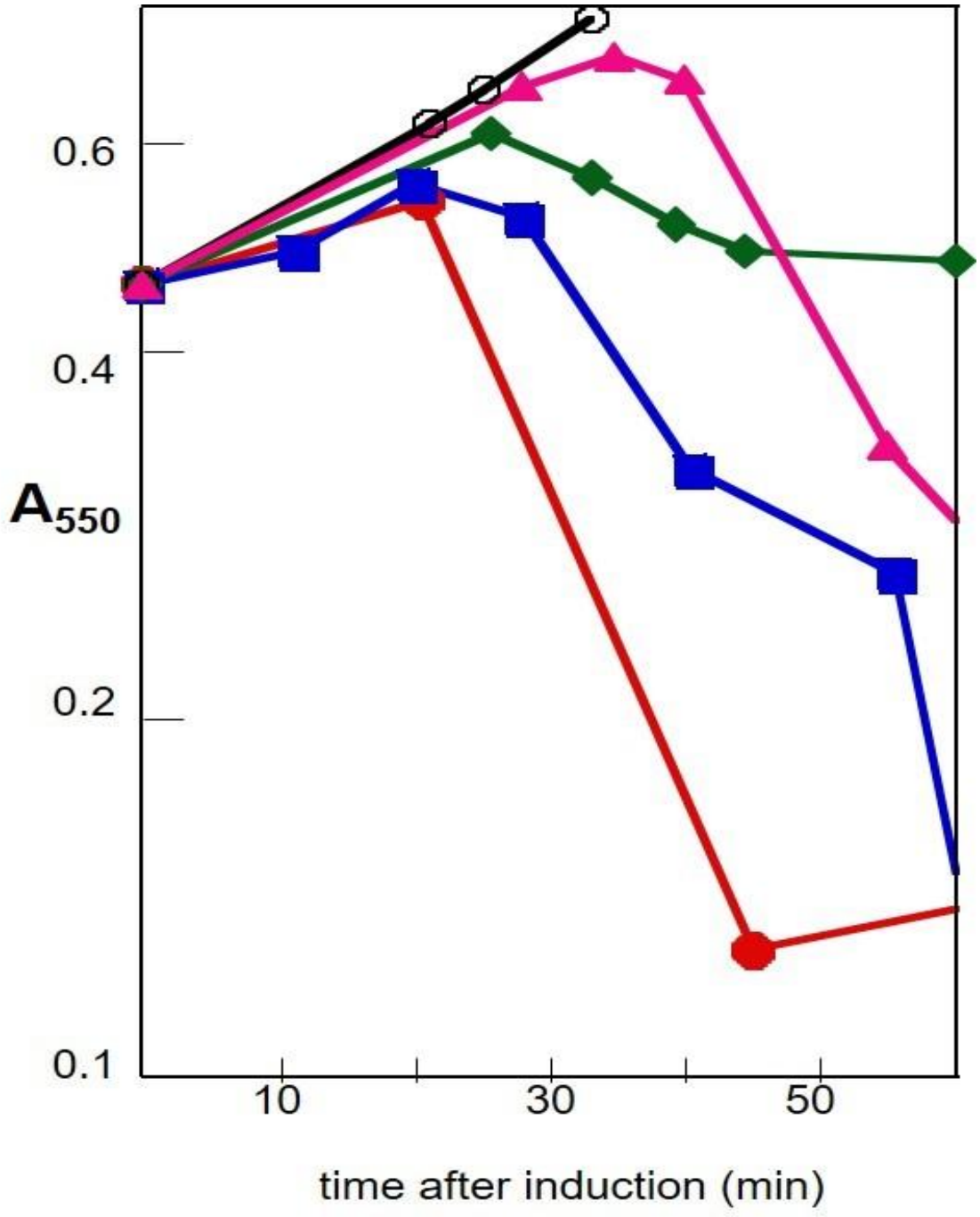

Figure S9. N-terminal fragments of A_2 can cause lysis of *E. coli*. Growth profiles of N-terminal fragments of A_2 as expressed in BL21(DE3) pLysS pET11a-(His)A_2. Induction of N-terminal fragments consisting of the first 190, 186 and 180 residues (red circles, blue squares, green diamonds respectively) but not 172 (black open circles) or fewer, cause lysis. Full length A_2 is shown (pink triangles). Culture turbidity indicating the cell lysis was monitored as a function of time.

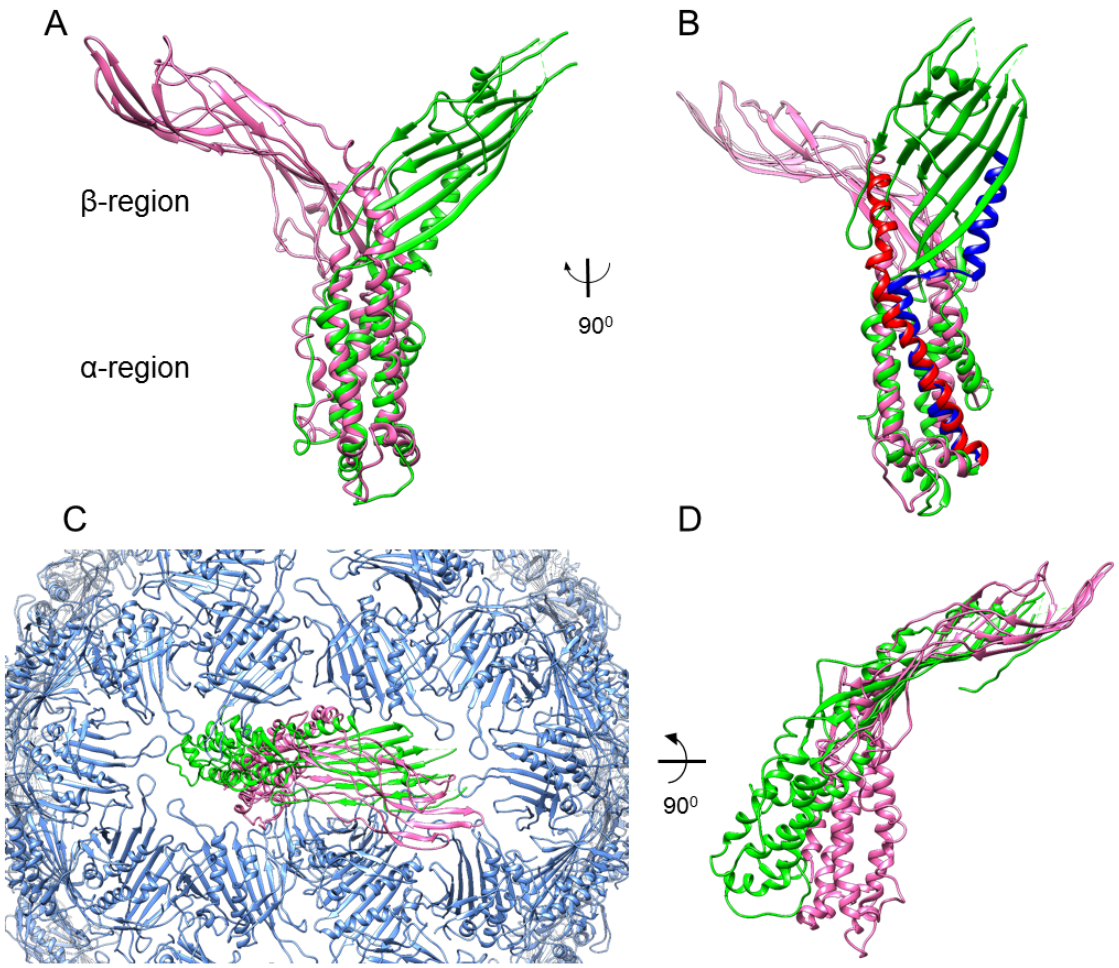

Figure S10. Structural comparison of the maturation proteins from Qβ and MS2. (A) The maturation protein, A protein, from MS2 (green, PDB ID: 5TC1) is aligned to the refined cryo-EM model of A_2 from Qβ (hot pink) based on their α-regions. (B) The long helix in A_2 and the helix-loop-helix in A that connect the α- and β-regions are colored red and blue, respectively. (C) The maturation proteins from MS2 and Qβ are aligned based on the their proximal coat protein dimers. For visualization only the capsid coat proteins from Qβ are shown (cornflower blue). (D) A 90° rotation with the capsid coat proteins removed shows the side view of the A and A_2 proteins, revealing that the α-regions of the two maturation proteins insert into their capsids at different angles.

Table S1. Statistics for the backbone model of the Qβ virion capsid, the atomic model of the Qβ VLP capsid and the pseudo-atomic model of the MurA-A_2 complex.

Model statistics	Backbone model of the Qβ virion capsid	Atomic model of the Qβ VLP capsid	Pseudo-atomic model of the MurA-A_2 complex
All-atom clash score	2.08	6.11	20.24
Ramachandran plot (%):			
outliers	0.00	0.00	0.24
allowed	6.12	7.94	7.2
favored	93.88	92.06	92.56
Rotamer outliers (%)	N/A	0.00	0.00
C-β deviations	N/A	0	0